

Magnetic Field Landscapes Guiding the Chemisorption of Diamagnetic Molecules

Florian Ahrend,^{†,§} Ulrich Glebe,^{‡,§,◆} Línay Árnadóttir,^{||,⊥,+} Joe E. Baio,^{||,⊥,+} Daniel A. Fischer,[#] Chernó Jaye,[#] Bonnie O. Leung,^{▽,■} Adam P. Hitchcock,[○] Tobias Weidner,^{||,⊥,||} Ulrich Siemeling,^{*,‡,§} and Arno Ehresmann^{*,†,§}

[†]Institute of Physics, University of Kassel, Heinrich-Plett-Str. 40, D-34132 Kassel, Germany

[‡]Institute of Chemistry, University of Kassel, Heinrich-Plett-Str. 40, D-34132 Kassel, Germany

[§]Center for Interdisciplinary Nanostructure Science and Technology (CINSaT), University of Kassel, Heinrich-Plett-Str. 40, D-34132 Kassel, Germany

^{||}National ESCA and Surface Analysis Center for Biomedical Problems (NESAC/BIO) Departments of Bioengineering and Chemical Engineering, University of Washington, Seattle, Washington 98195, United States

[⊥]Oregon State University, Corvallis, Oregon 97331, United States

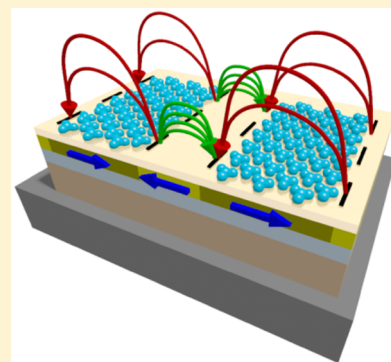
[#]National Institute of Standards and Technology, Gaithersburg, Maryland 20899, United States

[▽]Alberta Environment and Sustainable Resource Development, Edmonton, Alberta T5K 2J6, Canada

[○]Chemistry and Chemical Biology, BIMR, McMaster University Hamilton, Ontario L8S 4M1, Canada

Supporting Information

ABSTRACT: It is shown that the self-assembly of diamagnetic molecule submonolayers on a surface can be influenced by magnetic stray field landscapes emerging from artificially fabricated magnetic domains and domain walls. The directed local chemisorption of diamagnetic subphthalocyaninoboron molecules in relation to the artificially created domain pattern is proved by a combination of surface analytical methods: ToF-SIMS, X-PEEM, and NEXAFS imaging. Thereby, a new method to influence self-assembly processes and to produce patterned submonolayers is presented.



INTRODUCTION

Controlling the properties of surfaces and interfaces is a major challenge for the scientific and industrial communities. An attractive approach in this context is the use of self-assembled monolayers (SAMs).^{1–3} SAMs are 2D polycrystalline monomolecular films attached to suitable substrates, which can be fabricated from both solution and gas phases. For several applications, however, it is critical to deposit the surfactant into spatially defined regions of the substrate, avoiding the growth of a whole layer and providing desired functionalities in certain areas of interest. Such locally functionalized surfaces are of interest in the fields of nanoelectronics,⁴ spintronics,⁵ optoelectronics,⁶ or information storage.^{7,8} The formation of laterally patterned SAMs is demanding. It has previously been achieved by different lithographic and stamp techniques,^{9–12} by chemical surface modification,^{13,14} and by the application of electric fields.^{15,16} Magnetic fields, however, which were recently applied with great success to the controlled positioning of micro- and nanoparticles,¹⁷ have not been used as a tool for

molecular patterning in this context. This may be due to the expectation that magnetic forces exerted, for example, by magnetic domain walls of magnetically structured substrates being too weak in comparison to the energy of Brownian molecular motion in solution. However, the use of physical methods like external fields may be advantageous because the unspecific interaction leads to a manifold of systems that can be influenced. Here we show that it is possible to influence the positions of local chemisorption of diamagnetic molecular assemblies in submonolayers on a surface by local magnetic stray fields. This experimental finding together with the ability to fabricate artificial magnetic domain patterns¹⁸ with tailored magnetic domain wall charges (i.e., tailored magnetic stray fields)¹⁹ by light ion bombardment induced magnetic patterning (IBMP) results in a new technology, where

Received: July 18, 2016

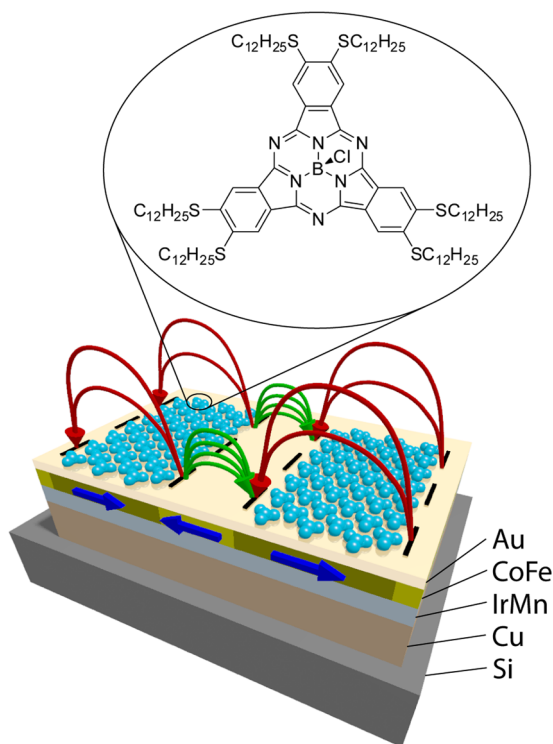
Revised: September 23, 2016

Published: September 23, 2016

diamagnetic molecules can be self-assembled at defined locations on a surface. We therefore expand the toolbox for local positioning of molecular material by a new and promising method that we expect to be highly applicable to different systems and to have a wide variety in the resulting molecular structures while being a cheap and fast way to produce micropatterns on a centimeter scale.

In detail, it will be shown that diamagnetic homologues of subphthalocyanine macrocycles, forming self-assembled monolayers on nonmagnetic gold surfaces,²⁰ are preferentially chemisorbed in areas of weakest magnetic flux density on a substrate artificially patterned into magnetic parallel-stripe domains of alternating widths, causing a lateral variation of the magnetic flux density over the surface (Scheme 1). The

Scheme 1. Schematic View of the Exchange-Biased Layer Stack, the Magnetic Pattern (Indicated by Straight Arrows), and Its Resulting Stray Fields above the Sample Surface (curved arrows)^a



^aCoFe: ferromagnetic layer, IrMn: antiferromagnetic layer. Additionally the distribution and the chemical structure of the subphthalocyanineboron complex [B(Subpc)(Sn-C₁₂H₂₅)₆] with an axial chlorido ligand and six peripheral *n*-dodecylthio substituents is shown.

directed local chemisorption of diamagnetic subphthalocyanineboron complex molecules in relation to the artificially created domain pattern will be proven by a combination of surface analytical methods: time-of-flight secondary ion mass spectrometry (ToF-SIMS), X-ray photoemission electron microscopy (X-PEEM), and near-edge X-ray absorption fine structure (NEXAFS) imaging.

■ SAMPLES WITH ARTIFICIAL MAGNETIC FIELD LANDSCAPES AND MOLECULE DEPOSITION

The layer systems used for the fabrication of artificial domain/domain wall patterns and, therefore, artificial magnetic stray

field landscapes are shown in Scheme 1. In brief, these are Si/Cu^{50nm}/Ir₁₇Mn₈₃^{10nm}/Co₇₀Fe₃₀^{5nm}/Au^{5-8nm} exchange-biased magnetic layer systems²¹ magnetically patterned by IBMP^{18,22} into magnetic parallel stripe domains with different stripe widths (for details, see the Experimental Methods). In remanence, these stripes possess head-to-head/tail-to-tail magnetization configurations in adjacent parallel stripe-domains. Magnetic flux densities over the narrower domains are higher than those over the wider domains. AFM characterizations of the surface did not show any structural difference between bombarded and nonbombarded areas. TEM measurements performed for a different layer system prior to and after a bombardment procedure did not show differences.²³ For the different surface characterization experiments, the samples were prepared in characterization-method-adapted ways: Samples for ToF-SIMS analysis were coated with an 8 nm thick Au cover layer (series 1), while the samples for the X-PEEM measurements were covered with a slightly thinner cover layer of 5 nm (series 2) to be able to detect photoelectrons emitted from the ferromagnetic layer below the gold cap. The magnetic domain structure for these samples consists of periodic stripe domains of alternating 3.5 and 6.5 μm widths. The spatial resolution of the NEXAFS imaging experiment is ~50 μm, and hence substrates with larger magnetic stripe domains with widths of 170 and 230 μm are used, while the thickness of the gold capping layer is again 8 nm (series 3). Adsorbate molecules [B(Subpc)(Sn-C₁₂H₂₅)₆] were deposited from dichloromethane solution. We previously found that SAMs of these molecules on pure gold substrates form during an immersion time of 12 h.²⁰ In contrast, an immersion time of only 1 min was used in the present experiments to limit the surface density of adsorbate molecules. Subsequently the samples were immersed without rinsing in pure dichloromethane for 12 h (for details of compound synthesis and deposition procedure, see the Experimental Methods).

■ RESULTS

ToF-SIMS Characterization. ToF-SIMS for surface studies^{24,25} possesses a high molecular sensitivity, surface sensitivity, and lateral resolution, which is ideally suited for the detection of low-concentration species such as molecules adsorbed in monolayers or submonolayers. ToF-SIMS images were therefore obtained from samples of series 1, which had been immersed in a 1 μM solution of the adsorbate molecules. The images resolved an area of 50 × 50 μm² with 256 × 256 pixels. A complete mass spectrum with ~400 peaks (for other details, see the Experimental Methods) was recorded at each pixel. The thin layer of adsorbate made it very challenging to directly image the stripes through the adsorbate molecular fragments, so additionally metal peaks with higher sensitivity and maximum autocorrelation factor (MAF)^{26,27} analysis were used. Figure 1 shows an image of the total ion counts and images showing the lateral distribution of the combined intensity of selected peaks, which were defined by the MAF analysis. The stripes are well visible in both positive and negative secondary ion spectra, but spots of contamination are only seen in the negative spectra (Figure 1a,b).

The total ion image (Figure 1a) shows two main features: well-formed lines and irregular spots. The spots showed high intensity of OH and are most likely due to contamination during sample preparation or shipping and are not of interest here. MAF analysis assisted in the further interpretation of the data. For the negative secondary ion image, the MAF analysis

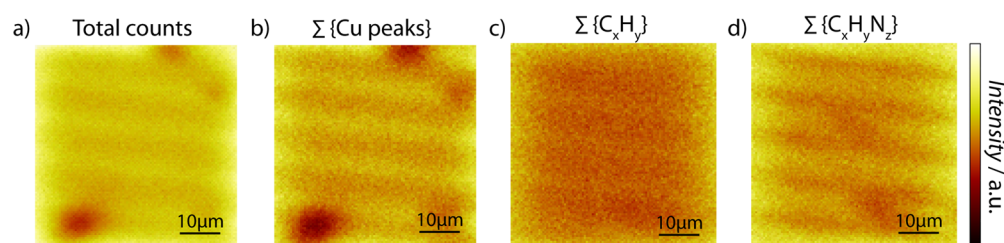


Figure 1. ToF-SIMS images of the adsorbed molecules. (a,b) Negative secondary ions and (c,d) positive secondary ions. All images are from the same spot of the sample. (a) Total ion image from the negative secondary ions. (b) Summation of the six highest MAF loadings listed in Table 1 corresponding to different Cu fragments. (c,d) Positive secondary ions images of the combined intensities of the carbon peaks (c) and nitrogen containing peaks (d) in Table 2. These group of peaks were identified through a MAF analysis.

grouped Cu- and Cl-related peaks from the underlying surface together, suggesting a difference in adsorbate concentration on the surface. Because Cu is a common contaminant in Au,²⁸ it seems like there is a low surface coverage in the Cu-rich areas. The peaks corresponding to the six highest loadings from this analysis listed in Table 1 and their lateral distribution are shown in Figure 1b.

Table 1. Peak Assignments for Highest Loadings for MAF Analysis for the Negative Secondary Ions Image

fragment	measured mass (u)
³⁷ Cl	36.967
⁶⁵ CuCl ₂	134.875
Cu ₂ H ₂ O ₂	159.862
⁶⁵ CuCuH ₂ O ₂	161.860
CuCl ₂	132.879
⁶⁵ Cu ³⁷ ClCl	136.8759

MAF analysis of the positive secondary ion image showed high contrast for salt contaminants, which have very high yield in ToF-SIMS experiments²⁰ and therefore are left out here, but also a separation of C_xH_y and C_xH_yN_z fragments appears. The two chemical groups load separately, C_xH_y negative and C_xH_yN_z positive, but the polarity has no meaning. The highest loadings for the C_xH_y and C_xH_yN_z fragments, respectively, are listed in Table 2, and the combined intensities of the peaks are shown in Figure 1c,d. While C_xH_y shows only slightly higher concentration in narrow stripes (Figure 1c), C_xH_yN_z shows stronger patterning in wider stripes between the areas of the hydrocarbons (Figure 1d). The nitrogen-containing hydro-

Table 2. Peak Assignments for Hydrocarbons (negative loadings) and Nitrogen-Containing Hydrocarbons (positive loadings) Given by MAF Analysis of the Positive Secondary Ion Image

negative loadings		positive loadings	
fragment	measured mass (u)	fragment	measured mass (u)
C ₃ H ₅	41.0400	C ₈ H ₁₅ N	125.1219
C ₃ H ₇	43.0579	C ₃ H ₈ N	58.0715
C ₄ H ₇	55.0604	C ₂ H ₄ N	56.0598
C ₂ H ₅	29.0402	C ₃ H ₆ N	43.0211
C ₂ H ₃	27.0242	C ₂ H ₃ O	123.1093
C ₄ H ₉	57.0771	C ₈ H ₁₃ N	124.1159
C ₅ H ₉	69.0815	C ₈ H ₁₄ N	73.0681
C ₂ H ₄	28.0324	C ₆ H ₁₅ N	109.0869
		C ₇ H ₁₁ N	56.0598

carbons represent the subphthalocyanine molecules, while the hydrocarbons are most likely due to contaminants. Because self-assembling species have the ability for self-cleaning effects, contaminants are mainly left in areas with low-molecule concentration. Because of the planar structure and the controlled deposition of the adsorbates with the molecular plane parallel to the sample surface,²⁰ mainly a monatomic layer of adsorbate material covers the surface, therefore showing an increased yield of Cu containing ions in the negative spectra appearing from the underlying gold layer. The fact that the axially bound chlorine atom is kept stable at the molecule structure during adsorption²⁰ explains the increased signal of Cl containing ions with the Cu fragments (see Table 1). In contrast, in the areas with low-molecule coverage a comparable thick layer of contaminants is left, reducing the signals of the substrate.

Therefore, the ToF-SIMS results indicate that the subphthalocyanine molecules grow in a periodicity matching to the periodicity of the magnetic pattern, with a preferential adsorption in broader stripes, whose width correlates with the width of the broader magnetic domains. Although this finding agrees well with classical theory, where diamagnets avoid spatial regions with high magnetic flux densities, it is surprising in terms of simple energetic considerations.

The Brownian energy of a particle at room temperature is in the range of $E_B = \frac{3}{2} \cdot k_b T \approx 10^{-21}$ J. Calculations of the out-of-plane magnetic field strength above the sample surface following the approach of Rugar et al.^{29,30} and an estimate of the magnetic susceptibility of the diamagnetic molecules by the use of Pascal's constants^{31,32} deliver magnetic interaction energies in the range of 10^{-31} J. Kinetic energies of the molecules due to their Brownian motion are therefore orders of magnitude larger than the estimate for their magnetic interaction energy with the artificial domain pattern of the substrate, rendering magnetic positioning of molecules from solution unlikely. Therefore, it was investigated whether an increased subphthalocyanine deposition in the wider domains might have occurred due to possible local surface modifications. Increased surface roughness or a modified surface chemistry may exist in areas modified by the ion bombardment or the surface chemistry may have been modified due to possible residual resist material from the magnetic patterning process. Because these effects would be the result of laterally changing surface characteristics, a special sample was prepared, where the magnetically patterned thin film system of series 1 was covered by an additional Au cover layer of 5 nm prior to molecule deposition. Possible surface modifications from the magnetic patterning process are therefore buried and should not influence the surface chemistry. For this sample, there is an

increased subphthalocyanine deposition measured by ToF-SIMS in the wider domains too (data not shown here).

Surface Characterization by X-PEEM. X-PEEM enables simultaneous characterization of the elemental distribution close to the surface and magnetic structure of the sample.^{33,34} Although the ToF-SIMS results already indicated a preferential self-assembly over the wider magnetic domains, we wanted to confirm in a direct experiment whether the molecules avoid self-assembly over each domain wall and the smaller domains, that is, areas of higher magnetic flux density. Figure 2a shows

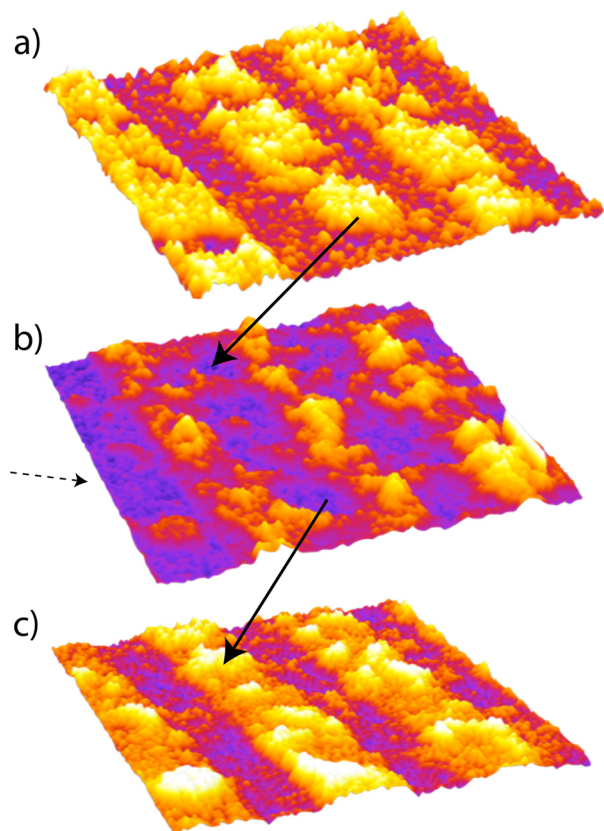


Figure 2. $30 \times 30 \mu\text{m}^2$ images of the X-PEEM measurements in a false color and 3D visualization. For raw data images and extracted NEXAFS spectra, see the [Supporting Information](#). (a) C $1s\text{-}\pi^*$ emission as a function of position, representative for the subphthalocyanine molecule distribution. (b) Iron L -edge emission after excitation by right-handed circularly polarized light at the same position of the sample. The exciting-photons impinged under 30° glancing angle from the direction as indicated by the dashed arrow. (c) Same as panel b but excitation with left handed circularly polarized light. Solid arrows point to the identical stripe of the substrate.

the electron yield after excitation of the C $1s\text{-}\pi^*$ resonances (284.6 to 285.5 eV) as a function of position of a magnetically patterned sample of series 2 being indicative for the chemisorbed subphthalocyaninatoboron complexes. Clearly, increased intensities are observed in wider stripes, in agreement with the results of the ToF-SIMS analyses. The underlying artificial magnetic domains are visualized by magnetic circular dichroism in photoemission at the iron L -edge using left or right circularly polarized light at the same spot of the sample like in Figure 2a (Figure 2b,c). As is obvious from this Figure, the macrocycles are deposited preferentially over the broader

magnetic domains and avoid self-assembly in the smaller domains.

Surface Characterization by Imaging NEXAFS. Finally, NEXAFS imaging measurements were carried out.^{35,36} Here the surface was imaged where each pixel contained a full NEXAFS spectrum. On the contrary, for each exciting-photon energy a laterally resolved image can be generated. This detection mode enables the selection of signals characteristic for particular resonances. Figure 3a shows the NEXAFS image

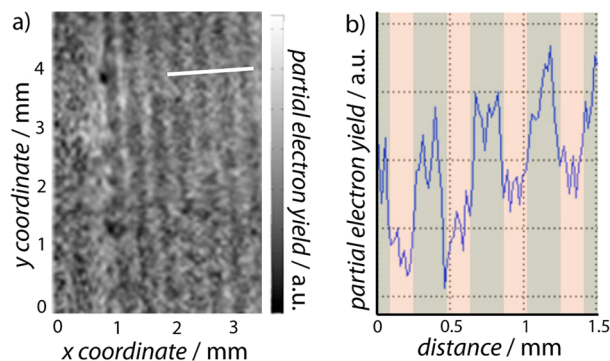


Figure 3. (a) NEXAFS image of a series 3 sample measured with imaging NEXAFS at the C $1s \rightarrow \pi^*$ resonance (285 eV excitation energy). Increased intensity of the π^* resonance is depicted with brighter contrast. (b) Partial electron yield at 285 eV along the marked line in panel a. The differently colored backgrounds indicate the width of the magnetic domain patterns.

of the π^* resonance of the carbon atoms in the aromatic units of the subphthalocyaninatoboron complex at 285 eV excitation energy. Again, a clear stripe-patterned distribution of the chemisorbed molecules is found, with a larger signal on the wider stripes. Figure 3b shows a scan of the line marked in Figure 3a, illustrating this finding. This experiment was also a final control experiment of whether a modified surface chemistry induced by the magnetic patterning process would have an influence on the self-assembly of the macrocycles. In contrast with the samples prepared for the ToF-SIMS and X-PEEM measurements (series 1 and 2), where the broader domains have been bombarded by He^+ ions, here the smaller domains were the modified ones by ion bombardment. Nevertheless the characterization results also indicate a preferred deposition of the subphthalocyaninatoboron complexes over the wider domains.

SUMMARY AND CONCLUSIONS

The analyses of the self-assembly of subphthalocyaninatoboron complexes $[\text{BClSubpc}'(\text{Sn-C}_{12}\text{H}_{25})_6]$ on magnetically parallel-stripe patterned surfaces by ToF-SIMS, X-PEEM, and NEXAFS imaging demonstrate a preferred deposition of the molecules over the wider domains of the substrate. This is in agreement with the classical picture of diamagnetic materials avoiding areas of high magnetic flux densities. This behavior is surprising because the kinetic energies of the molecules due to Brownian motion in solution are orders of magnitude larger than the magnetic energy gain when the molecules position themselves in response to the magnetic field. Surface diffusion of the molecules by statistical hopping of physisorbed molecules overlaid by a drift directed by the strong local field gradients and the sensitive interplay of different energies during the self-assembly process itself seems to play a decisive role. One may

speculate that the induced drift by this field gradient may cause increased nucleation centers for the chemisorption and self-assembly of the molecules in favorable areas. This hypothetical mechanism, however, will have to be corroborated in future experiments. With the presented finding, positions of self-assembling diamagnetic molecule adsorption can be controlled by magnetic field landscapes over a full substrate surface (range of cm^2) in a quick and cheap way.

EXPERIMENTAL METHODS

A sputtered exchange-bias thin-film layer system is magnetically patterned via IBMP with a home-built plasma ion source³⁷ in a head-to-head/tail-to-tail magnetized domain pattern. Details of the fabrication process can be found in the [Supporting Information](#), section 1.

[BClSubpc'(Sn-C₁₂H₂₅)₆] (Figure 1)³⁸ was synthesized following the route for its *n*-octylthio derivative.³⁹ The deposition of the adsorbate onto the magnetically patterned sample surfaces was performed from CH₂Cl₂ solution. Further information on the synthesis and deposition process can be found in the [Supporting Information](#), section 2.

ToF-SIMS data were collected on an ION-TOF 5-100 instrument using a Bi₃⁺² primary ion source. The exact parameters and calibration can be found in the [Supporting Information](#), section 3.

X-PEEM measurements were carried out at the Advanced Light Source (ALS) on bending magnet beamline 7.3.1.⁴⁰ X-PEEM data analysis was performed with the aXis2000 software package.⁴¹ Further information can be found in the [Supporting Information](#), section 4.

NEXAFS spectra were measured at the National Synchrotron Light Source (NSLS) U7A beamline at Brookhaven National Laboratory. Further information can be found in the [Supporting Information](#), section 5.

ASSOCIATED CONTENT

Supporting Information

The Supporting Information is available free of charge on the ACS Publications website at DOI: 10.1021/acs.langmuir.6b02208.

Section 1: Fabrication of artificial strayfield landscapes. Section 2: Synthesis, molecule description and preparation of submonolayers. Section 3: Time-of-flight secondary ion mass spectrometry (ToF-SIMS). Section 4: X-ray photoemission electron microscopy (X-PEEM). Section 5: Near-edge X-ray absorption fine structure (NEXAFS) imaging. Figure S1. X-PEEM images of series 2 sample. (PDF)

AUTHOR INFORMATION

Corresponding Authors

*A.E.: E-mail: ehresmann@physik.uni-kassel.de.

*U.S.: E-mail: siemeling@uni-kassel.de.

Present Addresses

◆U.G.: Fraunhofer-Institut für Angewandte Polymerforschung, Geiselbergstraße 69, 14476 Potsdam-Golm, Germany.

†T.W.: Max-Planck-Institute for Polymer Research, Ackermannweg 10, D-55128 Mainz, Germany.

†L.Á. and J.E.B.: School of Chemical, Biological and Environmental Engineering, Oregon State University, 1500 SW Jefferson Way, Corvallis 97331, Oregon.

■B.O.L.: University of British Columbia, 2329 West Mall, Vancouver, BC V6T 1Z4, Canada.

Author Contributions

The manuscript was written through contributions of all authors. All authors have given approval to the final version of the manuscript.

Notes

The authors declare no competing financial interest.

ACKNOWLEDGMENTS

U.G. thanks the Fonds der Chemischen Industrie for a doctoral fellowship. We thank David G. Castner for support of this work and Lara J. Gamble for collaboration. J.E.B. thanks the National Science Foundation for a research fellowship (NSF grant #1202620). L.Á. thanks IonToF for generously donating a software license to enable the ToF-SIMS analysis. We thank Andreas Scholl and Andrew Doran for assistance with the X-PEEM measurements. Data were acquired using PEEM-2 at ALS beamline 7.3.1, which is supported by the Director of the Office of Science, Department of Energy, under Contract No. DE-AC02-05CH11231. T.W., J.E.B., C.J., and D.A.F. acknowledge support for NEXAFS imaging experiments by the NSLS, Brookhaven National Laboratory, which is supported by the U.S. Department of Energy, Division of Materials Science and Division of Chemical Sciences. This work is also a part of the research program of the Max-Planck Society. Certain commercial names are used in this paper as examples and do not constitute an endorsement by the National Institute of Standards and Technology.

ABBREVIATIONS

SAMs, self-assembled monolayers; IBMP, ion bombardment induced magnetic patterning; ToF-SIMS, time-of-flight secondary ion mass spectrometry; X-PEEM, X-ray photoemission electron microscopy; NEXAFS, near-edge X-ray absorption fine structure

REFERENCES

- (1) Schreiber, F. Structure and growth of self-assembling monolayers. *Prog. Surf. Sci.* **2000**, *65*, 151.
- (2) Barth, J. V. Molecular architectonic on metal surfaces. *Annu. Rev. Phys. Chem.* **2007**, *58*, 375.
- (3) De Feyter, S.; De Schryver, F. C. Two-dimensional supramolecular self-assembly probed by scanning tunneling microscopy. *Chem. Soc. Rev.* **2003**, *32*, 139.
- (4) Carbone, C.; Gardonio, S.; Moras, P.; Lounis, S.; Heide, M.; Bihlmayer, G.; Atodiresei, N.; Dederichs, P. H.; Blügel, S.; Vlais, S.; Lehnert, A.; Ouazi, S.; Rusponi, S.; Brune, H.; Honolka, J.; Enders, A.; Kern, K.; Stepanow, S.; Krull, C.; Balashov, T.; Mugarza, A.; Gambardella, P. Self-assembled nanometer-scale magnetic networks on surfaces: Fundamental interactions and functional properties. *Adv. Funct. Mater.* **2011**, *21*, 1212.
- (5) Cavallini, M. Status and perspectives in thin films and patterning of spin crossover compounds. *Phys. Chem. Chem. Phys.* **2012**, *14*, 11867.
- (6) Matsuda, M.; Isozaki, H.; Tajima, H. Electroluminescence quenching caused by a spin-crossover transition. *Chem. Lett.* **2008**, *37*, 374.
- (7) Cavallini, M.; Biscarini, F.; Gomez-Segura, J.; Ruiz, D.; Veciana, J. Multiple length scale patterning of single-molecule magnets. *Nano Lett.* **2003**, *3*, 1527.
- (8) Krusin-Elbaum, L.; Shibauchi, T.; Argyle, B.; Gignac, L.; Weller, D. Stable ultrahigh-density magneto-optical recordings using introduced linear defects. *Nature* **2001**, *410*, 444.
- (9) Kim, K.; Ford, A.; Meenakshi, V.; Teizer, W.; Zhao, H.; Dunbar, K. R. Nanopatterning of Mn12-acetate single-molecule magnet films. *J. Appl. Phys.* **2007**, *102*, 094306.

- (10) Domingo, N.; Bellido, E.; Ruiz-Molina, D. Advances on structuring, integration and magnetic characterization of molecular nanomagnets on surfaces and devices. *Chem. Soc. Rev.* **2012**, *41*, 258.
- (11) Bernard, A.; Delamarche, E.; Schmid, H.; Michel, B.; Bosshard, H. R.; Biebuyck, H. Printing Patterns of Proteins. *Langmuir* **1998**, *14*, 2225.
- (12) Renault, J. P.; Bernard, A.; Bietsch, A.; Michel, B.; Bosshard, H. R.; Delamarche, E.; Kreiter, M.; Hecht, B.; Wild, U. P. Fabricating Arrays of Single Protein Molecules on Glass Using Microcontact Printing. *J. Phys. Chem. B* **2003**, *107*, 703.
- (13) Gatteschi, D.; Cornia, A.; Mannini, M.; Sessoli, R. Organizing and Addressing Magnetic Molecules. *Inorg. Chem.* **2009**, *48*, 3408.
- (14) Bonifazi, D.; Mohnani, S.; Llanes-Pallas, A. Supramolecular Chemistry at Interfaces: Molecular Recognition on Nanopatterned Porous Surfaces. *Chem. - Eur. J.* **2009**, *15*, 7004.
- (15) Suo, Z.; Hong, W. Programmable motion and patterning of molecules on solid surfaces. *Proc. Natl. Acad. Sci. U. S. A.* **2004**, *101*, 7874.
- (16) Zhang, Z.; Sharma, P.; Borca, C. N.; Dowben, P. A.; Gruverman, A. Polarization-specific adsorption of organic molecules on ferroelectric LiNbO₃ surfaces. *Appl. Phys. Lett.* **2010**, *97*, 243702.
- (17) Ennen, I.; Höink, V.; Weddemann, A.; Hütten, A.; Schmalhorst, J.; Reiss, G.; Waltenberg, C.; Jutzi, P.; Weis, T.; Engel, D.; Ehresmann, A. Manipulation of magnetic nanoparticles by the strayfield of magnetically patterned ferromagnetic layers. *J. Appl. Phys.* **2007**, *102*, 013910.
- (18) Fassbender, J.; Poppe, S.; Mewes, T.; Mougin, A.; Hillebrands, B.; Engel, D.; Jung, M.; Ehresmann, A.; Schmoranzler, H.; Faini, G.; Kirk, K. J.; Chapman, J. N. Magnetization reversal of exchange bias double layers magnetically patterned by ion irradiation. *Phys. status solidi a* **2002**, *189*, 439.
- (19) Holzinger, D.; Zingsem, N.; Koch, I.; Gaul, A.; Fohler, M.; Schmidt, C.; Ehresmann, A. Tailored domain wall charges by individually set in-plane magnetic domains for magnetic field landscape design. *J. Appl. Phys.* **2013**, *114*, 013908.
- (20) Glebe, U.; Baio, J. E.; Árnadóttir, L.; Siemeling, U.; Weidner, T. Molecular Suction Pads: Self-assembled monolayers of subphthalocyaninoboron complexes on gold. *ChemPhysChem* **2013**, *14*, 1155.
- (21) O'Grady, K.; Fernandez-Outon, L.; Vallejo-Fernandez, G. A new paradigm for exchange bias in polycrystalline thin films. *J. Magn. Magn. Mater.* **2010**, *322*, 883.
- (22) Ehresmann, A.; Engel, D.; Weis, T.; Schindler, A.; Junk, D.; Schmalhorst, J.; Höink, V.; Sacher, M. D.; Reiss, G. Fundamentals for magnetic patterning by ion bombardment of exchange bias layer systems. *Phys. Status Solidi B* **2006**, *243*, 29.
- (23) Ehresmann, A.; Junk, D.; Engel, D.; Paetzold, A.; Röhl, K. On the origin of ion bombardment induced exchange bias modifications in polycrystalline layers. *J. Phys. D: Appl. Phys.* **2005**, *38*, 801.
- (24) Belu, A. M.; Graham, D. J.; Castner, D. G. Time-of-flight secondary ion mass spectrometry: techniques and applications for the characterization of biomaterial surfaces. *Biomaterials* **2003**, *24*, 3635.
- (25) Benninghoven, A. Chemical Analysis of Inorganic and Organic Surfaces and Thin Films by Static Time-of-Flight Secondary Ion Mass Spectrometry (TOF-SIMS). *Angew. Chem., Int. Ed. Engl.* **1994**, *33*, 1023.
- (26) Tyler, B. J.; Rayal, G.; Castner, D. G. Multivariate analysis strategies for processing ToF-SIMS images of biomaterials. *Biomaterials* **2007**, *28*, 2412.
- (27) Larsen, R. Decomposition using maximum autocorrelation factors. *J. Chemom.* **2002**, *16*, 427.
- (28) Siemeling, U.; Schirmmayer, C.; Glebe, U.; Bruhn, C.; Baio, J. E.; Árnadóttir, L.; Castner, D. G.; Weidner, T. Phthalocyaninato complexes with peripheral alkylthio chains- Disk-like adsorbate species for the vertical anchoring of ligands onto gold surfaces. *Inorg. Chim. Acta* **2011**, *374*, 302.
- (29) Rugar, D.; Mamin, H. J.; Guethner, P.; Lambert, S. E.; Stern, J. E.; McFadyen, I.; Yogi, T. Magnetic force microscopy - General principles and application to longitudinal media. *J. Appl. Phys.* **1990**, *68* (3), 1169.
- (30) Potter, R. I. Analysis of Saturation Magnetic Recording Based on Arc tangent Magnetization Transitions. *J. Appl. Phys.* **1970**, *41*, 1647.
- (31) Bain, G. A.; Berry, J. F. Diamagnetic corrections and Pascals Constants. *J. Chem. Educ.* **2008**, *85*, 532.
- (32) Kumar, M.; Gupta, R. Landolt-Börnstein - Numerical data and functional relationships in science and technology, New series, Springer, 2007, Berlin, Heidelberg.
- (33) Locatelli, A.; Bauer, E. Recent advances in chemical and magnetic imaging of surfaces and interfaces by XPEEM. *J. Phys.: Condens. Matter* **2008**, *20*, 093002.
- (34) Yamaguchi, Y.; Takakusagi, S.; Sakai, Y.; Kato, M.; Asakura, K.; Iwasawa, Y. X-ray photoemission electron microscopy (XPEEM) as a new promising tool for the real-time chemical imaging of active surfaces. *J. Mol. Catal. A: Chem.* **1999**, *141*, 129.
- (35) Baio, J. E.; Jaye, C.; Fischer, D. A.; Weidner, T. Multiplexed orientation and structure analysis by imaging near-edge X-ray absorption fine structure (MOSAIX) for combinatorial surface science. *Anal. Chem.* **2013**, *85*, 4307.
- (36) Konicek, A. R.; Jaye, C.; Hamilton, M. A.; Sawyer, W. G.; Fischer, D. A.; Carpick, R. W. Near-edge X-ray absorption fine structure imaging of spherical and flat counterfaces of ultrananocrystalline diamond tribological contacts: A correlation of surface chemistry and friction. *Tribol. Lett.* **2011**, *44*, 99.
- (37) Lengemann, D.; Engel, D.; Ehresmann, A. Plasma ion source for in situ ion bombardment in a soft x-ray magnetic scattering diffractometer. *Rev. Sci. Instrum.* **2012**, *83*, 053303.
- (38) Ho Kang, S.; Kim, K.; Kang, Y.-S.; Zin, W.-C.; Olbrechts, G.; Wostyn, K.; Clays, K.; Persoons, A. Novel columnar mesogen with octupolar optical nonlinearities: synthesis, mesogenic behavior and multiphoton-fluorescence-free hyperpolarizabilities of subphthalocyanines with long aliphatic chains. *Chem. Commun.* **1999**, 1661.
- (39) Claessens, C. G.; González-Rodríguez, D.; del Rey, B.; Torres, T.; Mark, G.; Schuchmann, H.-P.; von Sonntag, C.; MacDonald, J. G.; Nohr, R. S. Highly efficient synthesis of chloro- and phenoxy-substituted subphthalocyanines. *Eur. J. Org. Chem.* **2003**, *2003*, 2547.
- (40) Anders, S.; Padmore, H. A.; Duarte, R. M.; Renner, T.; Stammer, T.; Scholl, A.; Scheinfein, M. R.; Stohr, J.; Seve, L.; Sinkovic, B. Photoemission electron microscope for the study of magnetic materials. *Rev. Sci. Instrum.* **1999**, *70*, 3973.
- (41) aXis2000 is free for non-commercial use, available from <http://unicorn.mcmaster.ca/aXis2000.html>.